Molecules and Cells

WWC1 and NF2 Prevent the Development of Intrahepatic Cholangiocarcinoma by Regulating YAP/TAZ Activity through LATS in Mice

Jaeoh Park[1], Jeong Sik Kim[1], Ji Hae Nahm[2,3], Sang-Kyum Kim[3], Da-Hye Lee[4,*], and Dae-Sik Lim[1,*]

[1]Department of Biological Sciences, National Creative Research Initiatives Center, Korea Advanced Institute of Science and Technology (KAIST), Daejeon 34141, Korea, [2]Department of Pathology, Yonsei University College of Medicine, Gangnam Severance Hospital, Seoul 06273, Korea, [3]Department of Pathology, Yonsei University College of Medicine, Severance Hospital Seoul, Seoul 03722, Korea, [4]Center for Bioanalysis, Korea Research Institute for Standards and Science, Daejeon 34113, Korea
*Correspondence: dahye.lee04@kriss.re.kr (DHL); daesiklim@kaist.ac.kr (DSL)
https://doi.org/10.14348/molcells.2020.0093
www.molcells.org

Hippo signaling acts as a tumor suppressor pathway by inhibiting the proliferation of adult stem cells and progenitor cells in various organs. Liver-specific deletion of Hippo pathway components in mice induces liver cancer development through activation of the transcriptional coactivators, YAP and TAZ, which exhibit nuclear enrichment and are activated in numerous types of cancer. The upstream-most regulators of Warts, the *Drosophila* ortholog of mammalian LATS1/2, are Kibra, Expanded, and Merlin. However, the roles of the corresponding mammalian orthologs, WWC1, FRMD6 and NF2, in the regulation of LATS1/2 activity and liver tumorigenesis *in vivo* are not fully understood. Here, we show that deletion of both *Wwc1* and *Nf2* in the liver accelerates intrahepatic cholangiocarcinoma (iCCA) development through activation of YAP/TAZ. Additionally, biliary epithelial cell-specific deletion of both *Lats1* and *Lats2* using a Sox9-Cre^{ERT2} system resulted in iCCA development through hyperactivation of YAP/TAZ. These findings suggest that WWC1 and NF2 cooperate to promote suppression of cholangiocarcinoma development by inhibiting the oncogenic activity of YAP/TAZ via LATS1/2.

Keywords: cholangiocarcinoma, Hippo pathway, NF2, WWC1, YAP

INTRODUCTION

Hippo signaling has been highlighted as a strong tumor-suppressor pathway (Choi et al., 2018; Yu et al., 2015). Components of the Hippo pathway, discovered initially in *Drosophila* through genetic screenings, are known to be well conserved in mammals. These mammalian orthologs (with *Drosophila* components in parentheses) are as follows: large tumor-suppressor kinase 1 and 2 [LATS1/2] (Wts), mammalian ste20-like kinase 1 and 2 [MST1/2] (Hpo), Salvador homolog 1 [SAV1] (Sav), neurofibromatosis type 2 [NF2] (Mer), MOB kinase activator 1A and B [MOB1A/B] (Mats), WW and C2 domain-containing 1, 2, and 3 [WWC1/2/3] (Kibra), and FERM-domain containing 6 [FRMD6] (Ex) (Baumgartner et al., 2010; Genevet et al., 2010; Halder and Johnson, 2011; Pan, 2007). LATS1/2 kinases phosphorylate the transcriptional coactivators, Yes-associated protein 1 (YAP) and WW-domain–containing transcription regulator 1 (TAZ) (Yki in *Drosophila*), thereby sequestering them in the cytoplasm and rendering them transcriptionally inactive. YAP and TAZ (YAP/TAZ) regulate genes related to lineage specification, self-renewal and the survival of various types of cells, including stem/progenitor cells (Camargo et al., 2007; Choi et al., 2018; Cordenonsi et al., 2011; Gregorieff et al., 2015; Ha-

Received 9 April, 2020; accepted 13 April, 2020; published online 15 May, 2020

eISSN: 0219-1032

yashi et al., 2015; Heallen et al., 2013; Moon et al., 2018).

To clarify the physiological roles and regulatory mechanism of the mammalian Hippo pathway, researchers have generated various tissue-specific knockout mice. In the liver, YAP not only serves as a critical factor during the development of bile ducts but also performs a decisive role during regeneration after liver damage (Lu et al., 2018; Zhang et al., 2010). Overexpression of active YAP results in enlargement of the liver with dysplastic changes in hepatocytes. Liver-specific knockout of the upstream components of the Hippo pathway, *Mst1/2*, *Sav1* or *Nf2*, induces the development of cancers with different histological features. Mice with liver-specific knockout of *Mst1/2* predominantly develop hepatocellular carcinoma (HCC) rather than intrahepatic cholangiocarcinoma (iCCA)(Song et al., 2010; Zhou et al., 2009). Ablation of *Mob1a/b* in the mouse liver induces the development of mixed HCC/iCCA, as does *Nf2* or *Sav1* knockout. In addition, loss of either of these genes also causes different degrees of progenitor cell expansion (Benhamouche et al., 2010; Lee et al., 2010; Nishio et al., 2016; Song et al., 2010). Although NF2 has been shown to regulate LATS1/2 *in vitro* through binding to WWC1, *Wwc1* single-knockout mice do not show any abnormal liver phenotypes (Makuch et al., 2011). However, *Wwc1/Wwc2* double knockout causes development of mixed HCC/iCCA within 1 year (Hermann et al., 2018), suggesting that other regulators are involved in the suppression of tumorigenesis to compensate the loss of WWC1. These previous results suggest that full activation of LATS cannot be achieved through WWC1 alone. Therefore, we hypothesized that WWC1 promotes activation of LATS through cooperation with NF2 in mammals, much as the complex of Kibra and Mer regulates and activates Hpo in *Drosophila* (Su et al., 2017). Here, we generated liver-specific *Nf2* and *Wwc1* double-knockout mice; notably, these mice died of iCCA at 3 to 4 weeks of age. To more specifically study the cellular origin of YAP activation-driven iCCA, we also generated mice in which both *Lats1* and *Lats2* were deleted only in biliary epithelial cells using a Sox9-Cre^{ERT2} system. Using these mice, we found that loss of *Lats1/2* rapidly leads to iCCA development through YAP/TAZ activation. Therefore, our findings suggest that WWC1 and NF2 act cooperatively to regulate LATS1/2-YAP in biliary epithelial cells of the liver and function as strong tumor suppressors on the path to iCCA development.

MATERIALS AND METHODS

Mice

Wwc1$^{-/-}$, *Nf2*$^{fl/fl}$, *Lats1*$^{fl/fl}$, *Lats2*$^{fl/fl}$, albumin-Cre transgenic (Tg) mice (B6.Cg-Tg(Alb-Cre)21Mgn/J), and Sox9-Cre^{ERT2} Tg ((Sox9-Cre/ERT2)1Msan/J) (JAX 018829) have been previously described (Giovannini et al., 2000; Heallen et al., 2011; 2013; Kim et al., 2013; Kopp et al., 2011; Makuch et al., 2011). *Wwc1*$^{-/-}$ (B6.129S6(Cg)-Wwc1tm1.1Rlh/J, 0244) and Sox9-Cre^{ERT2} mice were obtained from The Jackson Laboratory (USA). All mice were housed in a specific pathogen-free facility with a temperature- and light-controlled environment. Experiments with mice were performed according to guidelines of the Institutional Animal Care and Use Committee (IACUC) of the Korea Advanced Institute of Science and Technology (KAIST) (No. KA2010-23). *Wwc1*$^{-/-}$, *Nf2*$^{fl/fl}$, and albumin-Cre mice were sacrificed when moribund for histological and molecular analyses. Four to eight week-old male *Lats1*$^{fl/fl}$, *Lats2*$^{fl/fl}$, and Sox9-Cre^{ERT2} mice were induced with a single dose of tamoxifen (125 mg/kg) and later sacrificed for analyses.

Histological, immunohistochemical and immunofluorescence staining

Mice were perfused with phosphate-buffered saline (PBS) and their liver tissues were harvested and fixed by incubating with 10% formalin overnight at 4°C. After paraffin embedding, liver tissue blocks were cut into 4-μm-thick sections for H&E, immunohistochemical (IHC), and immunofluorescence (IF) staining. Deparaffinized and rehydrated sections were subjected to antigen retrieval in citrate buffer (10 mM tri-sodium citrate, 0.05% Tween 20, pH 6.0), after which endogenous peroxidase was blocked by incubating with 1% H_2O_2 for 10 min. Sections were then incubated in blocking buffer (3% bovine serum albumin and 0.3% Triton X-100 in PBS) at room temperature, followed by incubation overnight at 4°C with primary antibodies (Supplementary Table S1). After washing for 30 min to remove primary antibody, sections were incubated with horseradish peroxidase (HRP)-conjugate secondary antibodies at room temperature for 1 h, and then washed thoroughly again to remove secondary antibodies. Sections were then developed using a DAB Substrate Kit (Vector Laboratories, USA), and nuclei were counterstained with hematoxylin. N-cadherin and S100P were stained using a VENTANA BenchMark System (Roche Diagnostics, Switzerland).

For IF staining, the same procedure as above was performed, excluding the H_2O_2 blocking step, and fluorescent secondary antibodies were used instead of HRP-conjugated secondary antibodies (Supplementary Table S1). All antibodies were diluted in blocking buffer.

Reverse transcription PCR and quantitative PCR

Total RNA was isolated from homogenized liver tissues using easy-Blue Total RNA Extraction Kit (iNtRON Biotechnology, Korea). cDNA was then synthesized from 2 μg of total RNA with M-MLV reverse transcriptase (Enzynomics, Korea) using a mixture of oligo dT and random hexamers, according to the manufacturer's instructions. Quantitative polymerase chain reaction (qPCR) was performed on a CFX Connect Thermocycler (Bio-Rad, USA) using SYBR Green 2X Premix (Enzynomics) and the primers are listed in Supplementary Table S2.

Immunoblotting

Total protein was isolated from liver tissues using a lysis buffer (50 mM Tris-Cl pH 7.5, 150 mM NaCl, 0.1% SDS, 0.5% sodium deoxycholate, and 1 mM EDTA) containing protease and phosphatase inhibitors (1 mM NaF, 1 mM Na_3OV_4, phenylmethylsulfonyl fluoride [PMSF], leupeptin, and pepstatin; all from Sigma, USA) for 30 min on ice. After measuring the concentration of protein in lysates using a Pierce BCA protein assay kit (Thermo Fisher Scientific, USA), lysates containing equal amounts of protein (15 μg) were resolved by sodium dodecyl sulfate-polyacrylamide gel electrophore-

sis (SDS-PAGE). After transferring proteins to nitrocellulose membranes, blots were incubated overnight at 4°C with primary antibodies. After washing for 30 min with Tris-buffered saline (TBS) containing 0.1% Tween-20 (0.1% TBS-T), blots were incubated with secondary antibodies, diluted in TBS-T containing 5% skim milk. Blots were washed for 30 min with 0.1% TBS-T and then developed using ECL Westsave Gold (Abfrontier, Korea).

Human tissue array staining

Human normal tissue arrays (BN501a) and tissue arrays of different stages of liver iCCA (LV1004) were purchased from US Biomax (USA). Slides were incubated at 60°C for 1 h, after which immunohistochemistry was performed on a VENTANA BenchMark System using anti-YAP (1:100; Santa Cruz Biotechnology, USA) and anti-NF2 (1:200; Sigma) antibodies.

Statistical analysis

Graphing and statistical analyses (paired two-tailed Student's *t*-test and two-tailed Fisher's exact test) were performed using GraphPad Prism 6 software (GraphPad Software, USA).

RESULTS

Concurrent deletion of *Wwc1* and *Nf2* in the liver accelerates iCCA development in mice

To investigate potential cooperativity between NF2 and WWC1 in mammals, we crossed albumin-Cre mice with *Nf2*$^{fl/fl}$ and *Nf2*$^{fl/fl}$;*Wwc1*$^{-/-}$ mice to generate liver-specific *Nf2* single-knockout and *Nf2*; *Wwc1* double-knockout mice. Remarkably, these *Nf2*$^{fl/fl}$;*Wwc1*$^{-/-}$;albumin-Cre (hereafter, Nf2;Wwc1 DKO) mice showed severe cachexia and abdominal distension within 2 weeks after birth; their livers were also enlarged and presented large tumor nodules; in contrast, no changes were observed in livers of *Wwc1*$^{-/-}$ (hereafter, Wwc1 KO) mice (Fig. 1A). As previously reported, *Nf2*-deficient livers (*Nf2*$^{fl/fl}$;albumin-Cre, hereafter Nf2 KO) showed a slight increase in size at a time when Nf2;Wwc1 DKO livers exhibited obvious tumor nodules (Fig. 1B). Autophosphorylation of LATS was also dramatically decreased in Nf2;Wwc1 DKO mice (Fig. 1C). A histopathological analysis of H&E-stained slides of Nf2;Wwc1 DKO livers confirmed the development of iCCA, but not HCC (Figs. 1D and 1E). To further confirm iCCA development in the Nf2;Wwc1 DKO liver, we performed co-IF staining for the cholangiocyte and hepatocyte markers, cytokeratin 19 (CK19) and hepatocyte nuclear factor 4a (HNF4a), respectively (Fig. 1F). The Nf2;Wwc1 DKO liver exhibited high-grade cancer with malignant atypic cells, whereas the Nf2 KO liver showed minor expansion of cholangiocytes, which did not undergo dysplastic changes at the time point analyzed. Extensive desmoplastic reactions composed of a large number of fibroblasts surrounding the tumor were also observed in Nf2;Wwc1 DKO livers (Fig. 1G). Ultimately, Nf2;Wwc1 DKO mice died of iCCA within 3-4 weeks.

Increased YAP/TAZ activity promotes early development of iCCA in the Nf2;Wwc1 DKO liver

In line with the Western blotting results (Fig. 1C), IHC staining for YAP and TAZ in livers of 2-week-old control, Nf2 KO, Wwc1 KO, and Nf2;Wwc1 DKO mice revealed activation of YAP/TAZ in mutant livers. Indeed, some hepatocytes in Nf2 KO livers also showed nuclear YAP, and most hepatocytes and atypical tumor cells from Nf2;Wwc1 DKO livers were strongly positive for YAP and TAZ (Figs. 2A and 2B). Furthermore, these atypical tumor cells in periportal regions in Nf2;Wwc1 DKO livers were highly proliferative compared with those in the Nf2 KO liver, which showed moderate proliferation (Fig. 2C).

Only Nf2;Wwc1 DKO livers showed significant downregulation of hepatocyte-related genes together with upregulation of cholangiocyte-related genes (Fig. 2D). As expected, the upregulation of YAP target genes was more pronounced in Nf2;Wwc1 DKO livers than in other mutant livers (Fig. 2D). The fibrosis-related genes, *Vim* and *Col1a1*, were also moderately increased in the Nf2;Wwc1 DKO liver. Taken together, these results reveal the redundant and compensatory relationship between NF2 and WWC1 that regulates YAP/TAZ activity to prevent iCCA development.

Biliary epithelial cell-specific deletion of *Lats1/2* in mice promotes iCCA development

Many liver-specific knockout mouse models of Hippo components commonly show over-proliferation of biliary/progenitor cells, which further develops into HCCs or mixed HCC/iCCA (characteristics of both HCC and iCCA) (Benhamouche et al., 2010; Lee et al., 2010; Nishio et al., 2016; Zhang et al., 2010). Since knockout of Hippo components in these studies was achieved using an albumin-Cre system, which is expressed in hepatoblasts during embryonic liver development and continues to hepatocytes in the adult liver, both hepatic progenitor cells and dedifferentiated transformed hepatocytes might contribute to the development of mixed HCC/iCCA. Intriguingly, Nf2;Wwc1 DKO mice developed iCCA, but not HCC or mixed HCC/iCCA, unlike previously documented knockout mice lacking liver-specific expression of Hippo components. Therefore, to ascertain whether activation of YAP specifically in intrahepatic cholangiocytes drives iCCA development, we generated a biliary epithelial cell (BEC)-specific *Lats1/2* double-knockout mouse model by crossing Sox9-Cre^{ERT2} mice with a *Lats1*$^{fl/fl}$;*Lats2*$^{fl/fl}$ mouse model (*Lats1*$^{fl/fl}$;*Lats2*$^{fl/fl}$;Sox9 Cre^{ERT2}; hereafter, BEC-specific Lats1/2 DKO). We further crossed these mice with *R26-Tdtomato* reporter mice to trace the lineage of *Lats1/2* deleted cells.

Upon BEC-specific deletion of *Lats1/2* at 4 weeks of age, BEC-specific Lats1/2 DKO mice showed severe jaundice, which changed the color of the liver to yellow. Although tiny nodules were detectable on the surface of the BEC-specific Lats1/2 DKO liver, the liver itself showed no marked increase in size. A histopathological examination of H&E-stained sections revealed atypical, dysplastic biliary epithelial cancer cells within the BEC-specific Lats1/2 DKO liver (Fig. 3A). IHC staining for YAP and TAZ showed increased staining intensities within iCCA lesions, and immunostaining for Ki67 confirmed their proliferative feature (Fig. 3A). Co-IF staining for CK19 and tdTomato in BEC-specific Lats1/2 DKO mice revealed that CK19^{+} cells originated from *Lats1/2*-depleted BECs, and not from hepatocytes (Fig. 3B). Moreover, co-IF staining for CK19 and HNF4a further supported the interpretation that iCCAs

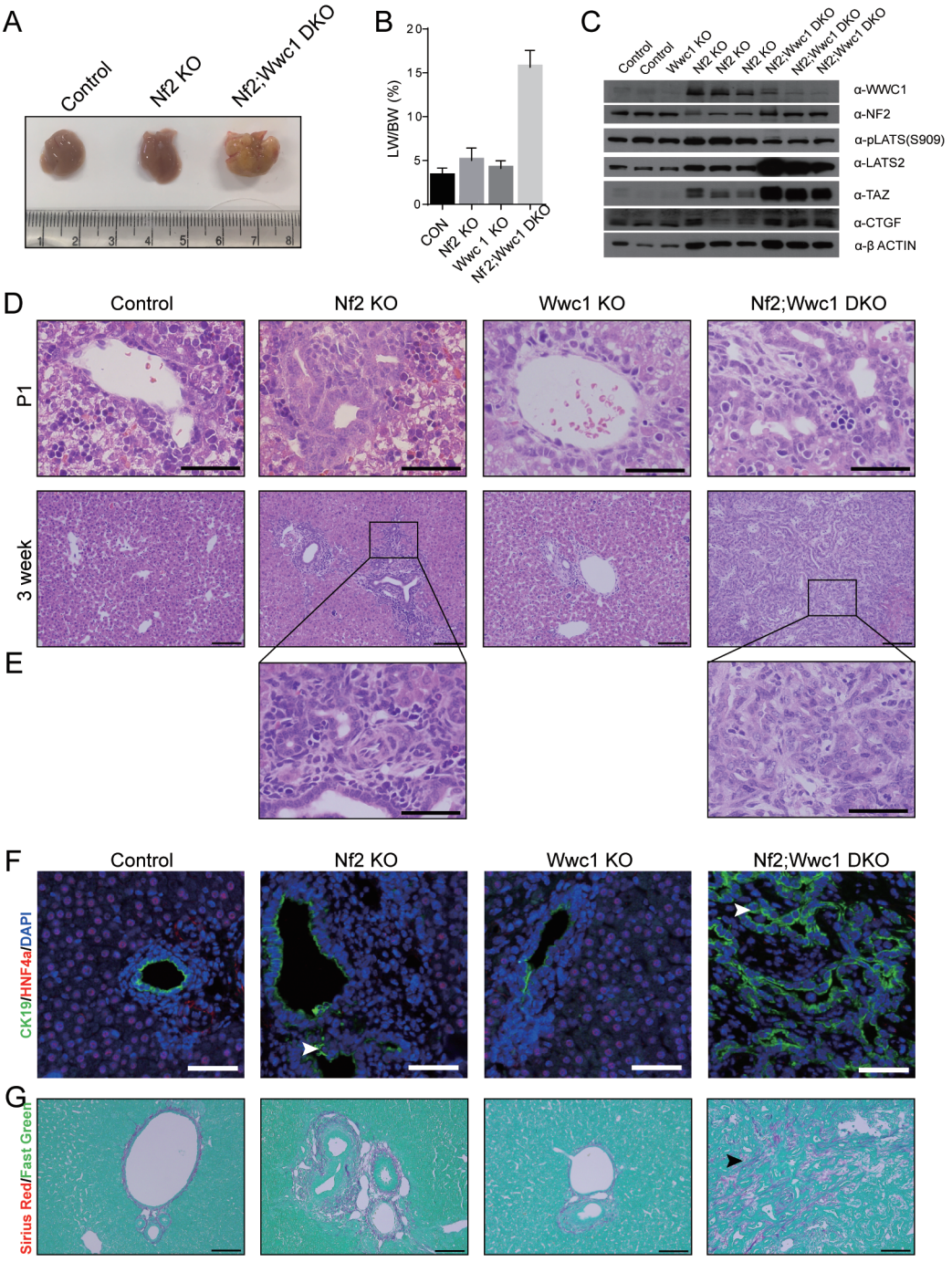

Fig. 1. Loss of NF2 and WWC1 in the liver induces iCCA. (A) Images of livers from 2-week-old control, Nf2 KO, and Nf2;Wwc1 DKO mice. (B) Ratio of liver weight (LW) to body weight (BW) for each genotype. (C) Western blot analysis of liver lysates from each mouse genotype. (D) Representative images of H&E-stained livers from each genotype of mice at postnatal day 1 (upper row; scale bars = 25 μm) and postnatal week 3 (lower row; scale bars = 100 μm). (E) Magnifications of images in panel D (scale bars = 25 μm). (F) Images of co-IF staining with antibodies against CK19 and HNF4a (white arrowheads indicate cholangiocytes; scale bars = 50 μm). (G) Images of Sirius red/Fast green staining in livers of 2-week-old mice (black arrowheads indicate accumulated collagen stained with Sirius Red; scale bars = 100 μm).

that developed in the BEC-specific Lats1/2 DKO liver are truly derived from BECs (Fig. 3B). Sirius Red staining was also increased, reflecting the expansion of fibroblastic cells in the BEC-specific Lats1/2 DKO liver (Fig. 3C). As expected, expression levels of YAP target genes were significantly increased in the BEC-specific Lats1/2 DKO liver (Fig. 3D). On the basis of

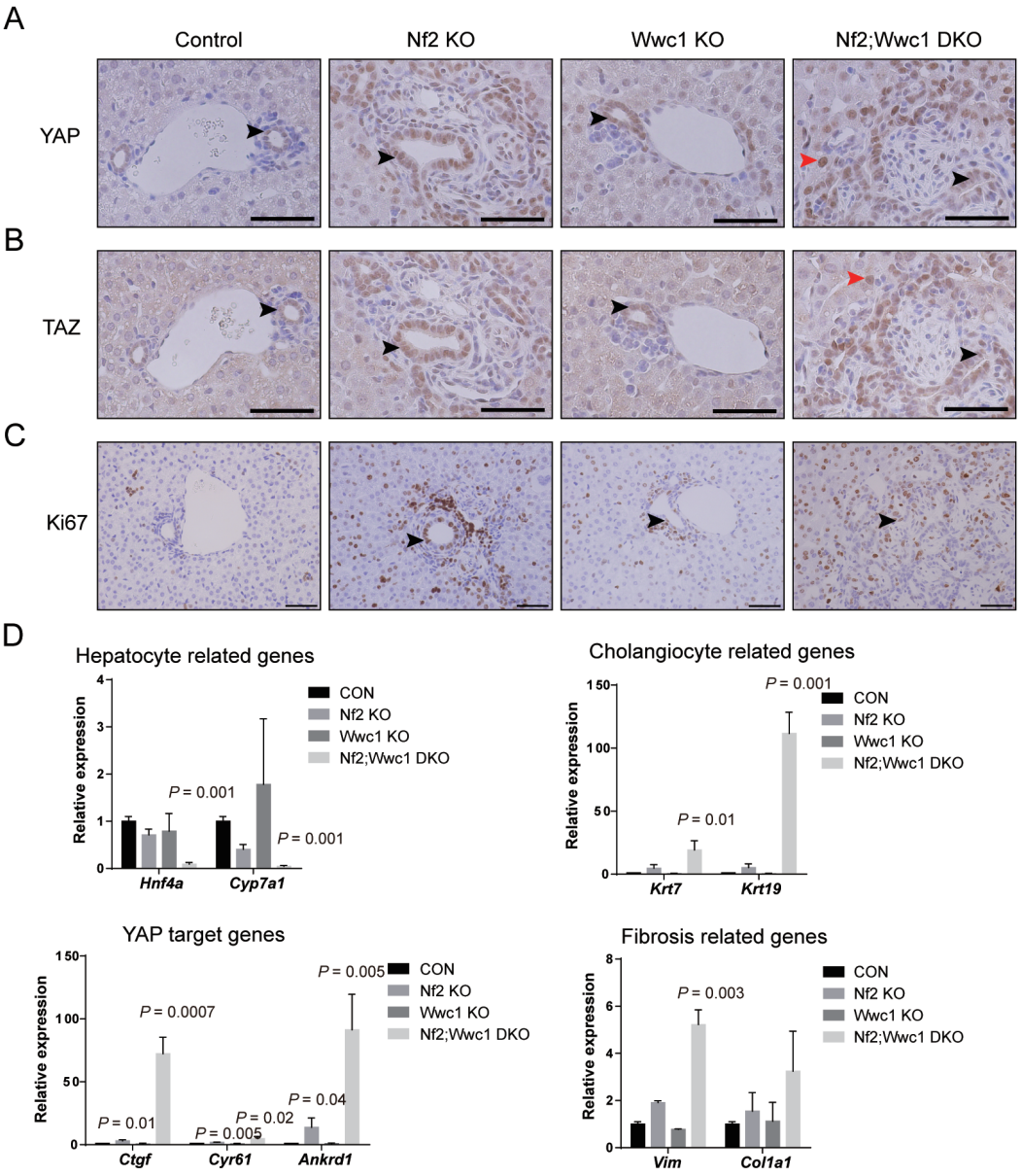

Fig. 2. YAP/TAZ are highly activated in both NF2- and WWC1-deficient cells. (A-C) Images of IHC staining with antibodies against YAP (A), TAZ (B), and Ki67 (C) in livers of 2-week-old mice (black and red arrowheads indicate cholangiocytes and hepatocytes, respectively; scale bars = 25 μm). (D) mRNA expression levels of hepatocyte related genes (*Hnf4a* and *Cyp7a1*), cholangiocyte-related genes (*Krt7* and *Krt19*), YAP target genes (*Cyr61*, *Ctgf*, *Ankrd1*), and fibrosis related genes (*Vim* and *Col1a1*) in livers of 2- to 3-week-old mice.

these results, we conclude that *Lats1/2* deletion in intrahepatic BECs leads to iCCA development through activation of YAP/TAZ in the liver.

iCCAs that develop in knockout mice lacking Hippo pathway components resemble human iCCAs

Human iCCA has been categorized into types 1 and 2 based on mucin productivity and immunophenotypes (Hayashi et al., 2016). In the present work, Alcian-blue staining of iCCAs in both Nf2;Wwc1 DKO and BEC-specific Lats1/2 DKO livers revealed very small amounts of mucin components, indicating that the tumors of both genotypes are composed of low-mucin–producing cancer cells (Fig. 4A). S100 calcium-binding protein P (S100P) immunostaining was faint in these cancer cells, but was high in non-epithelial cells of iCCAs that developed in Nf2;Wwc1 DKO and BEC-specific Lats1/2 DKO mice (Fig. 4B). We further found that BEC-specific Lats1/2 DKO and Nf2;Wwc1 DKO cancer cells adopted mesenchymal characteristics, as evidenced by positive staining for N-cadherin (Fig. 4C). Collectively, these data strongly support the conclusion that iCCAs that develop in Nf2;Wwc1 DKO and BEC-specific Lats1/2 DKO livers are similar to type 2 iCCA in human patients.

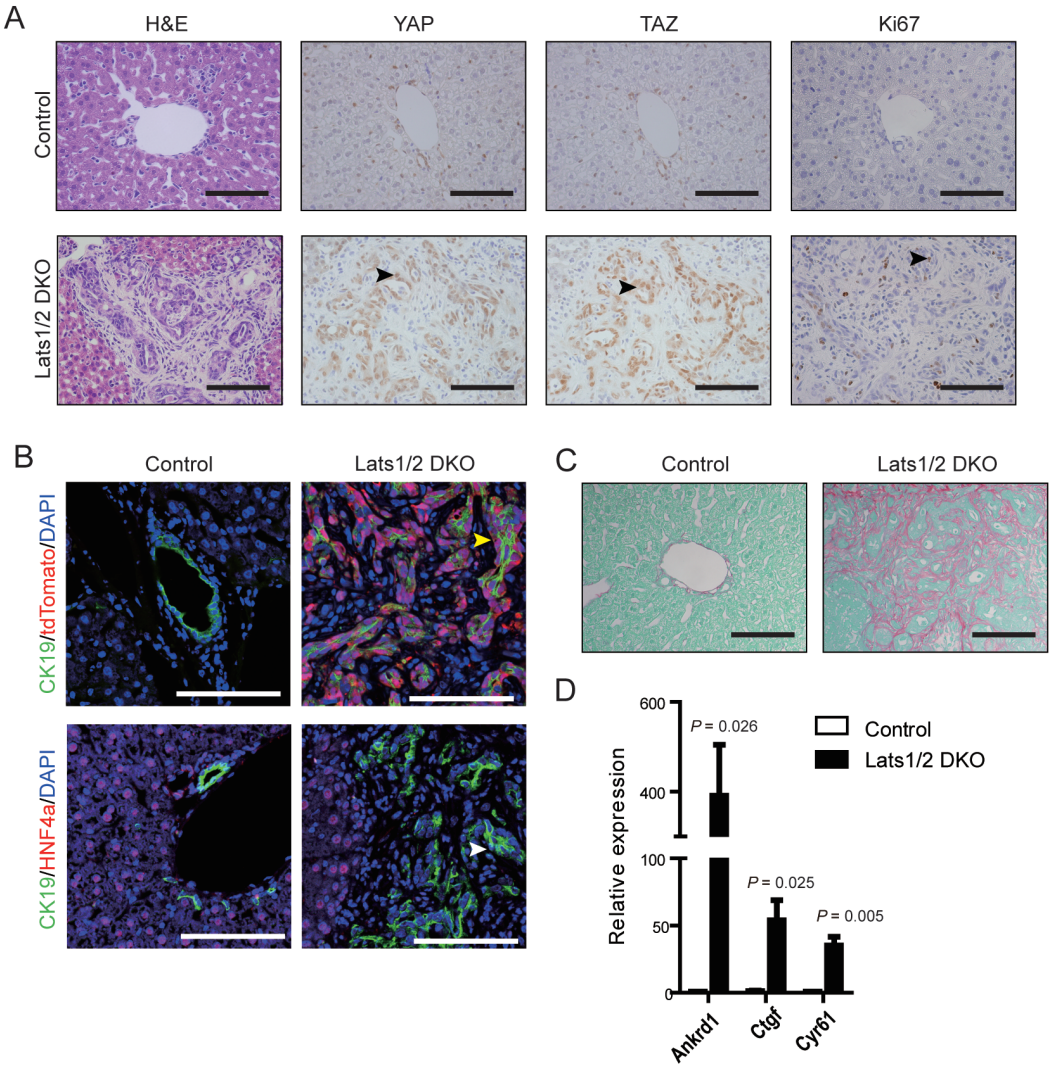

Fig. 3. Biliary cell-specific depletion of LATS1/2 leads to iCCA development. (A) Representative images of H&E staining and IHC staining with antibodies against YAP, TAZ, and Ki67 in the liver of BEC-specific Lats1/2 DKO mice (black arrowheads indicate cholangiocytes; scale bars = 50 μm). (B) Images of co-IF staining with antibodies against CK19 and HNF4a (yellow arrowhead indicates $CK19^{+}$/$tdTomato^{+}$ cells and white arrowhead indicates $CK19^{+}$/$HNF4^{-}$ cells; scale bars = 50 μm). (C) Images of Sirius red/Fast green staining in livers of BEC-specific Lats1/2 DKO mice (scale bars = 50 μm). (D) mRNA expression levels of the YAP target genes (*Ankrd1*, *Ctgf* and *Cyr61*) in livers of BEC-specific Lats1/2 DKO mice.

Expression of NF2 and YAP in human iCCA specimens

Previous studies have shown that YAP is highly active in human liver cancers (Marti et al., 2015; Rhee et al., 2018; Rizvi et al., 2018). Since both Nf2;Wwc1 DKO and BEC-specific Lats1/2 DKO mice developed iCCAs through activation of YAP/TAZ, we next sought to assess the expression of NF2, WWC1, LATS1/2 and YAP in human iCCA specimens. We found that NF2 was expressed in both hepatocytes and cholangiocytes, whereas YAP was predominantly detected in cholangiocytes in the human liver, as was the case in mouse liver (Fig. 5A) (Lee et al., 2016). Next, we examined the correlation between NF2 and YAP expression in immunostained human iCCA specimens and found that 67% of iCCA samples (10 of 15) that were negative for NF2 showed high levels of nuclear YAP staining. However, among the 26 samples positive for NF2 immunostaining, 13 were negative for nuclear YAP (Figs. 5B and 5C). Unfortunately, antibodies against LATS1/2 and WWC1 appropriate for IHC staining in normal human liver tissues were not commercially available; thus, expression of these components could not be tested in human specimens. Taken together, these results indicate that the expression of NF2 and YAP show an inverse correlation in human iCCA specimen.

DISCUSSION

HCC development has been relatively well studied, with genetic mouse models of HCC outnumbering those for iCCA.

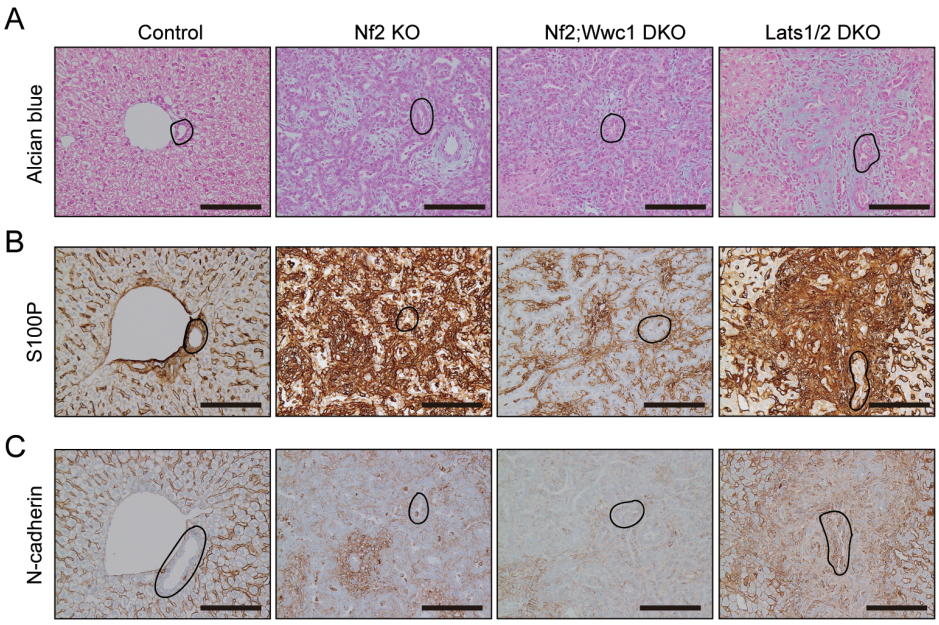

Fig. 4. iCCAs that develop in Nf2;Wwc1 DKO and BEC-specific Lats1/2 DKO livers resemble type 2 iCCA in human patients. (A-C) Representative images of Alcian-blue staining (A), IHC staining for S100P (B), and N-cadherin (C) in livers of 2- to 3-week-old mice of each genotype. Black circles indicate the ductular area in cancer (scale bars = 100 μm).

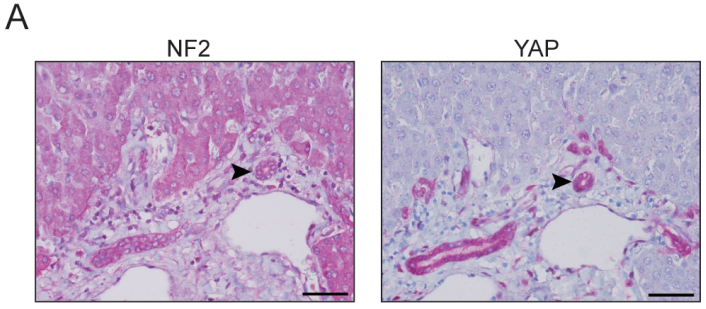

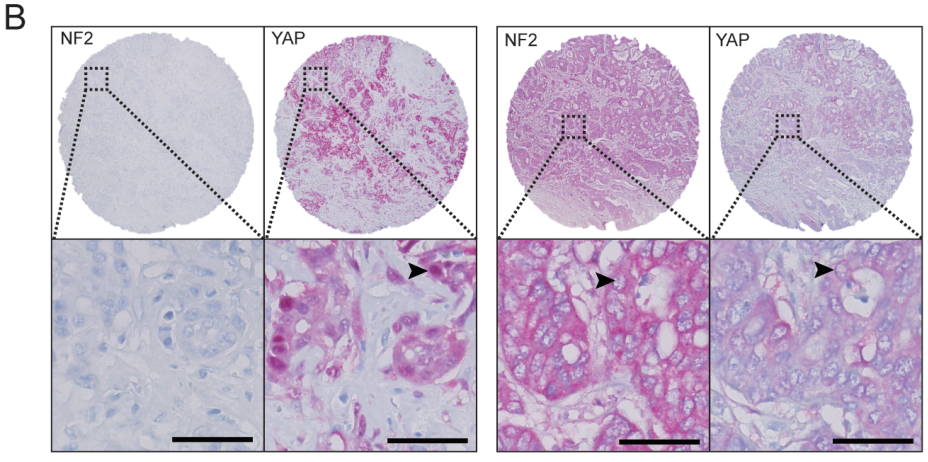

C

Nf2		YAP	
Negative	Positive	Cytoplasm	Nuclear
15		5	10
	26	13	13
41		18	23

Fig. 5. IHC staining for NF2 and YAP in human iCCA. (A and B) Representative images of IHC staining with antibodies against NF2 and YAP in normal (A) and iCCA (B) tissues (black arrowheads indicate cholangiocytes; scale bars = 25 μm). (C) Table of NF2 and YAP staining scores (one-tailed P = 0.2401, Fisher's exact test).

These studies, which highlighted the development of HCCs or mixed HCC/iCCA following albumin-Cre mediated perturbation of the Hippo pathway, led to the discovery of Hippo signaling as a tumor-suppressor pathway for liver cancers in mice. Although hyperactivation of YAP/TAZ in mice leads to the conversion of hepatocytes into BEC-like cells upon albumin-Cre or adeno-Cre-mediated loss of *Lats1* and *Lats2* in livers, iCCAs do not develop in these mouse models (Lee et al., 2016). Here, for the first time, we demonstrated iCCA development through activation of YAP/TAZ in both Nf2;Wwc1 DKO and BEC-specific Lats1/2 DKO mice, establishing that YAP activation specifically in intrahepatic cholangiocytes drives early onset of iCCA in mice.

The NF2/WWC1/FRMD6 complex is the most upstream element in the Hippo signaling pathway. Here, we found a drastic decrease in LATS activity in Nf2;Wwc1 DKO mice compared with mice with liver deletion of either *Wwc1* or *Nf2* alone. These results reflect the cooperative regulation of LATS activity *in vivo* by the two mammalian upstream Hippo pathway components, NF2 and WWC1. Nf2;Wwc1 DKO mice also showed marked acceleration of iCCA development compared with Nf2 KO mice. As was previously reported, deletion of *Wwc1* alone did not induce the development of liver cancer. Therefore, we suggest that WWC1 acts as a limiting factor rather than a necessary factor in regulating the activity of LATS. Additionally, given that WWC1, which serves as part of a negative feedback loop in the Hippo pathway, is a prime target of YAP activation, YAP activation may further potentiate the role of WWC1 as a 'brake'—a key factor in determining sustained activity of the Hippo pathway (Park et al., 2016). The cooperative actions of NF2 and WWC1, revealed by their loss in Nf2;Wwc1 DKO mice, is also supported by a recent report that MORC2, a DNA methyltransferase, mediates silencing of *NF2* and *WWC1* in human HCCs (Wang et al., 2018). Collectively, these findings provide direct evidence that NF2 and WWC1 synergize to prevent the development of YAP/TAZ-driven iCCA by regulating the activation of LATS1/2.

In human liver cancer patients, both HCC and iCCA tumors highly express YAP and TAZ (Van Haele et al., 2019), and YAP activity correlates with poor prognosis of patients, metastatic potential, and chromosomal instabilities of iCCAs (Marti et al., 2015; Pei et al., 2015; Rizvi et al., 2018). Thus, we sought to establish a correlation between YAP and NF2 expression in human iCCA samples. Although the majority of NF2-negative patients were positive for nuclear YAP, significant *p*-values were not obtained because the number of specimens was too small. There might be additional explanations for these limitations. First, unlike the case in HCCs, NF2 expression is not fully repressed in iCCAs (Wang et al., 2018) and is upregulated by YAP/TAZ activation owing to negative feedback (Park et al., 2016). Second, we could not estimate NF2 activity by IHC. Finally, no WWC1 antibody suitable for IHC staining is commercially available; thus, we could not determine whether expression levels of NF2 and WWC1 are correlated with nuclear YAP in human iCCA tissue microarrays.

In summary, we provide direct evidence that YAP/TAZ activation by deletion of *Nf2* and *Wwc1* or BEC-specific deletion of *Lats1* and *2* induces iCCA development in mice. Therefore, NF2, WWC1, and LATS1 and -2 act synergistically to prevent iCCA development by repressing YAP/TAZ activities in the bile duct compartment.

Note: Supplementary information is available on the Molecules and Cells website (www.molcells.org).

ACKNOWLEDGMENTS

This work was supported by grants from the National Creative Research Initiative Program (2010-0018277 to D.S.L.), the Korean Advanced Institute of Science and Technology (N11190050 to D.S.L.), the Individual Basic Science & Engineering Research Program (NRF-2016R1D1A1B03935764 to D.H.L.), and Establishment of measurement standards for Chemistry and Radiation funded by Korea Research Institute of Standards and Science (KRISS – 2020 – GP2020-0003, to D.H.L.).

AUTHOR CONTRIBUTIONS

D.S.L. and D.H.L. designed and led the study; D.H.L. and J.P. performed the experiments, analyzed the data, and wrote the manuscript; J.S.K. generated mouse model; J.H.N. diagnosed mouse liver tissues and S.K.K. analyzed patient samples. All authors read and approved the final manuscript.

CONFLICT OF INTEREST

The authors have no potential conflicts of interest to disclose.

ORCID

Jaeoh Park https://orcid.org/0000-0003-2699-371X
Jeong Sik Kim https://orcid.org/0000-0002-7389-8072
Ji Hae Nahm https://orcid.org/0000-0003-0902-866X
Sang-Kyum Kim https://orcid.org/0000-0003-0768-9923
Da-Hye Lee https://orcid.org/0000-0003-0580-9573
Dae-Sik Lim https://orcid.org/0000-0003-2356-7555

REFERENCES

Baumgartner, R., Poernbacher, I., Buser, N., Hafen, E., and Stocker, H. (2010). The WW domain protein Kibra acts upstream of Hippo in Drosophila. Dev. Cell *18*, 309-316.

Benhamouche, C.M., Saotome, I., Gladden, A.B., Liu, C.H., Giovannini, M., and McClatchey, A.I. (2010). Nf2/Merlin controls progenitor homeostasis and tumorigenesis in the liver. Genes Dev. *24*, 1718-1730.

Camargo, F.D., Gokhale, S., Johnnidis, J.B., Fu, D., Bell, G.W., Jaenisch, R., and Brummelkamp, T.R. (2007). YAP1 increases organ size and expands undifferentiated progenitor cells. Curr. Biol. *17*, 2054-2060.

Choi, W., Kim, J., Park, J., Lee, D.H., Hwang, D., Kim, J.H., Ashktorab, H., Smoot, D., Kim, S.Y., Choi, C., et al. (2018). YAP/TAZ initiates gastric tumorigenesis via upregulation of MYC. Cancer Res. *78*, 3306-3320.

Cordenonsi, M., Zanconato, F., Azzolin, L., Forcato, M., Rosato, A., Frasson, C., Inui, M., Montagner, M., Parenti, A.R., Poletti, A., et al. (2011). The Hippo transducer TAZ confers cancer stem cell-related traits on breast cancer cells. Cell *147*, 759-772.

Genevet, A., Wehr, M.C., Brain, R., Thompson, B.J., and Tapon, N. (2010). Kibra is a regulator of the Salvador/Warts/Hippo signaling network. Dev. Cell *18*, 300-308.

Giovannini, M., Robanus-Maandag, E., van der Valk, M., Niwa-Kawakita, M., Abramowski, V., Goutebroze, L., Woodruff, J.M., Berns, A., and Thomas, G. (2000). Conditional biallelic Nf2 mutation in the mouse promotes

manifestations of human neurofibromatosis type 2. Genes Dev. *14*, 1617-1630.

Gregorieff, A., Liu, Y., Inanlou, M.R., Khomchuk, Y., and Wrana, J.L. (2015). Yap-dependent reprogramming of Lgr5(+) stem cells drives intestinal regeneration and cancer. Nature *526,* 715-718.

Halder, G. and Johnson, R.L. (2011). Hippo signaling: growth control and beyond. Development *138*, 9-22.

Hayashi, A., Misumi, K., Shibahara, J., Arita, J., Sakamoto, Y., Hasegawa, K., Kokudo, N., and Fukayama, M. (2016). Distinct clinicopathologic and genetic features of 2 histologic subtypes of intrahepatic cholangiocarcinoma. Am. J. Surg. Pathol. *40*, 1021-1030.

Hayashi, S., Yokoyama, H., and Tamura, K. (2015). Roles of Hippo signaling pathway in size control of organ regeneration. Dev. Growth Differ. *57*, 341-351.

Heallen, T., Morikawa, Y., Leach, J., Tao, G., Willerson, J.T., Johnson, R.L., and Martin, J.F. (2013). Hippo signaling impedes adult heart regeneration. Development *140*, 4683-4690.

Heallen, T., Zhang, M., Wang, J., Bonilla-Claudio, M., Klysik, E., Johnson, R.L., and Martin, J.F. (2011). Hippo pathway inhibits Wnt signaling to restrain cardiomyocyte proliferation and heart size. Science *332*, 458-461.

Hermann, A., Wennmann, D.O., Gromnitza, S., Edeling, M., Van Marck, V., Sudol, M., Schaefer, L., Duning, K., Weide, T., Pavenstadt, H., et al. (2018). WW and C2 domain-containing proteins regulate hepatic cell differentiation and tumorigenesis through the hippo signaling pathway. Hepatology *67*, 1546-1559.

Kim, M., Kim, M., Lee, S., Kuninaka, S., Saya, H., Lee, H., Lee, S., and Lim, D.S. (2013). cAMP/PKA signalling reinforces the LATS-YAP pathway to fully suppress YAP in response to actin cytoskeletal changes. EMBO *J. 32*, 1543-1555.

Kopp, J.L., Dubois, C.L., Schaffer, A.E., Hao, E., Shih, H.P., Seymour, P.A., Ma, J., and Sander, M. (2011). Sox9+ ductal cells are multipotent progenitors throughout development but do not produce new endocrine cells in the normal or injured adult pancreas. Development *138*, 653-665.

Lee, D.H., Park, J.O., Kim, T.S., Kim, S.K., Kim, T.H., Kim, M.C., Park, G.S., Kim, J.H., Kuninaka, S., Olson, E.N., et al. (2016). LATS-YAP/TAZ controls lineage specification by regulating TGFbeta signaling and Hnf4alpha expression during liver development. Nat. Commun. *7*, 11961.

Lee, K.P., Lee, J.H., Kim, T.S., Kim, T.H., Park, H.D., Byun, J.S., Kim, M.C., Jeong, W.I., Calvisi, D.F., Kim, J.M., et al. (2010). The Hippo-Salvador pathway restrains hepatic oval cell proliferation, liver size, and liver tumorigenesis. Proc. Natl. Acad. Sci. U. S. A. *107*, 8248-8253.

Lu, L., Finegold, M.J., and Johnson, R.L. (2018). Hippo pathway coactivators Yap and Taz are required to coordinate mammalian liver regeneration. Exp. Mol. Med. *50*, e423.

Makuch, L., Volk, L., Anggono, V., Johnson, R.C., Yu, Y., Duning, K., Kremerskothen, J., Xia, J., Takamiya, K., and Huganir, R.L. (2011). Regulation of AMPA receptor function by the human memory-associated gene KIBRA. Neuron *71*, 1022-1029.

Marti, P., Stein, C., Blumer, T., Abraham, Y., Dill, M.T., Pikiolek, M., Orsini, V., Jurisic, G., Megel, P., Makowska, Z., et al. (2015). YAP promotes proliferation, chemoresistance, and angiogenesis in human cholangiocarcinoma through TEAD transcription factors. Hepatology *62*, 1497-1510.

Moon, K.H., Kim, H.T., Lee, D., Rao, M.B., Levine, E.M., Lim, D.S., and Kim, J.W. (2018). Differential expression of NF2 in neuroepithelial compartments is necessary for mammalian eye development. Dev. Cell *44*, 13-28.e3.

Nishio, M., Sugimachi, K., Goto, H., Wang, J., Morikawa, T., Miyachi, Y., Takano, Y., Hikasa, H., Itoh, T., Suzuki, S.O., et al. (2016). Dysregulated YAP1/TAZ and TGF-beta signaling mediate hepatocarcinogenesis in Mob1a/1b-deficient mice. Proc. Natl. Acad. Sci. U. S. A. *113*, E71-E80.

Pan, D. (2007). Hippo signaling in organ size control. Genes Dev. *21*, 886-897.

Park, G.S., Oh, H., Kim, M., Kim, T., Johnson, R.L., Irvine, K.D., and Lim, D.S. (2016). An evolutionarily conserved negative feedback mechanism in the Hippo pathway reflects functional difference between LATS1 and LATS2. Oncotarget *7*, 24063-24075.

Pei, T., Li, Y., Wang, J., Wang, H., Liang, Y., Shi, H., Sun, B., Yin, D., Sun, J., Song, R., et al. (2015). YAP is a critical oncogene in human cholangiocarcinoma. Oncotarget *6*, 17206-17220.

Rhee, H., Ko, J.E., Chung, T., Jee, B.A., Kwon, S.M., Nahm, J.H., Seok, J.Y., Yoo, J.E., Choi, J.S., Thorgeirsson, S.S., et al. (2018). Transcriptomic and histopathological analysis of cholangiolocellular differentiation trait in intrahepatic cholangiocarcinoma. Liver Int. *38*, 113-124.

Rizvi, S., Fischbach, S.R., Bronk, S.F., Hirsova, P., Krishnan, A., Dhanasekaran, R., Smadbeck, J.B., Smoot, R.L., Vasmatzis, G., and Gores, G.J. (2018). YAP-associated chromosomal instability and cholangiocarcinoma in mice. Oncotarget *9*, 5892-5905.

Song, H., Mak, K.K., Topol, L., Yun, K., Hu, J., Garrett, L., Chen, Y., Park, O., Chang, J., Simpson, R.M., et al. (2010). Mammalian Mst1 and Mst2 kinases play essential roles in organ size control and tumor suppression. Proc. Natl. Acad. Sci. U. S. A. *107*, 1431-1436.

Su, T., Ludwig, M.Z., Xu, J., and Fehon, R.G. (2017). Kibra and Merlin activate the Hippo pathway spatially distinct from and independent of Expanded. Dev. Cell *40*, 478-490.e3.

Van Haele, M., Moya, I.M., Karaman, R., Rens, G., Snoeck, J., Govaere, O., Nevens, F., Verslype, C., Topal, B., Monbaliu, D., et al. (2019). YAP and TAZ heterogeneity in primary liver cancer: an analysis of its prognostic and diagnostic role. Int. J. Mol. Sci. *20*, 638.

Wang, T., Qin, Z.Y., Wen, L.Z., Guo, Y., Liu, Q., Lei, Z.J., Pan, W., Liu, K.J., Wang, X.W., Lai, S.J., et al. (2018). Epigenetic restriction of Hippo signaling by MORC2 underlies stemness of hepatocellular carcinoma cells. Cell Death Differ. *25*, 2086-2100.

Yu, F.X., Zhao, B., and Guan, K.L. (2015). Hippo pathway in organ size control, tissue homeostasis, and cancer. Cell *163*, 811-828.

Zhang, N., Bai, H., David, K.K., Dong, J., Zheng, Y., Cai, J., Giovannini, M., Liu, P., Anders, R.A., and Pan, D. (2010). The Merlin/NF2 tumor suppressor functions through the YAP oncoprotein to regulate tissue homeostasis in mammals. Dev. Cell *19*, 27-38.

Zhou, D., Conrad, C., Xia, F., Park, J.S., Payer, B., Yin, Y., Lauwers, G.Y., Thasler, W., Lee, J.T., Avruch, J., et al. (2009). Mst1 and Mst2 maintain hepatocyte quiescence and suppress hepatocellular carcinoma development through inactivation of the Yap1 oncogene. Cancer Cell *16*, 425-438.